

Organo-modified mesoporous silica for sorption of carbon dioxide

Mária Badaničová · Vladimír Zelenák

Received: 16 December 2009 / Accepted: 17 March 2010 / Published online: 9 April 2010
© Springer-Verlag 2010

Abstract Organo-modified mesoporous silica SBA-15 has been studied for sorption of carbon dioxide (CO₂). The SBA-15 sample was functionalized with a branched chain polymer, polyethylenimine (PEI), of different molecular weights (1,300 and 2,000 g mol⁻¹). Surface modification was carried out by impregnation of silica by PEI or by grafting with (3-chloropropyl)triethoxysilane, followed by substitution of chlorine atoms by PEI ligands. The prepared modified mesoporous materials were characterized by nitrogen adsorption/desorption at 77 K, high-resolution transmission electron microscopy, small-angle X-ray scattering, and thermal methods. Sorption of CO₂ was studied by gravimetric method at 303 K. The total amount of sorbed CO₂ varied between 0.19–0.67 mmol/g for respective samples. Regeneration of the materials after adsorption was achieved by thermal treatment at 343 K.

Keywords Mesoporous silica · SBA-15 · Polyethylenimine · Adsorption · Carbon dioxide

Introduction

Greenhouse gases such as carbon dioxide have attracted great attention from the scientific community in recent years because they are supposed to be the major cause of global warming and climate change [1–4]. According to the results of periodic atmospheric measurements, various studies have been published regarding the increasing concentration of CO₂ in the atmosphere [5]. The results of

these studies have started discussions about the necessity to reduce the amount of CO₂ created and emitted through human activities. Sorption of CO₂ from flue gas appears to be one of the possible ways to reduce greenhouse gas emissions to the atmosphere.

Separation and sequestration of CO₂ is a complex technological process consisting of three steps: capture of gas, transport, and storage of captured gas [6, 7]. According to the study of Wong and Bioletti [8], the costs for capture and separation are the main limiting factor for large-scale capture of carbon dioxide produced by industry. Therefore, there is great demand for the development of cheap and easily regenerable sorbents for reduction of CO₂ emissions.

The development of new adsorbents for selective separation of CO₂ from gas mixtures is required also for purification of technologically important gases such as natural gas or hydrogen. Purification of hydrogen is of special interest, because it is considered that hydrogen technologies will play a key role in the near future. Since carbon dioxide is a byproduct in the technological production of hydrogen, e.g., by steam reforming of natural gas or in Syngas, effective and selective separation of CO₂ from H₂ is needed.

At present, separation of CO₂ in industry is achieved by CO₂ sorption in solutions of liquid amines. This technology is widespread because of its high selectivity. However, this approach suffers from several drawbacks such as corrosive behavior or expensive regeneration of sorbent [9, 10].

Amine-modified mesoporous silica provides a possibility to overcome such drawbacks. Leal et al. [11] studied silica gel grafted by 3-aminopropyl groups. Their infrared (IR) studies showed that adsorption of CO₂ over the material involves formation of ammonium carbamate under anhydrous conditions. In the presence of water each

M. Badaničová (✉) · V. Zelenák
Department of Inorganic Chemistry, P. J. Šafárik University,
Moyzesova 11, Košice, Slovak Republic
e-mail: maria.badanicova@student.upjs.sk

amino group can capture one molecule of CO₂, leading to the formation of ammonium bicarbonate. They reported CO₂ adsorption capacity of 0.45 mmol/g of adsorbent.

The adsorption properties of mesoporous silica MCM-48 grafted by 3-aminopropyltriethoxysilane were studied by Huang et al. [12]. The adsorption capacities in dry conditions were 1.14 mmol/g of sorbent. If the sorbent was exposed to a humid stream of 5% CO₂/N₂, the CO₂ adsorption capacity was doubled. On the contrary Hiyoshi et al., studying SBA-15 modified by (3-trimethoxysilylpropyl)dimethylenetriamine [13], found that the sorption capacities under anhydrous and hydrous conditions were comparable at 333 K.

Adsorption properties of MCM-48 modified by aminopropyl, pyrrolidinepropyl, polymerized aminopropyl, and polyethylenimine (PEI) were studied by Kim et al. [14]. The results showed the highest CO₂ adsorption rate for MCM-48 modified by aminopropyl (AP), because of greater availability of amine adsorption sites. The sorption capacity of AP-MCM-48 was 0.8 mmol/g. AP-MCM-48 has also showed high selectivity in separation of CO₂/N₂.

The effect of amine basicity on sorption properties was also studied [15]. SBA-12 mesoporous silica was modified by 3-aminopropyl (AP), 3-(methylamino)propyl (MAP), and 3-(phenylamino)propyl (PAP). The electronic effect in AP, MAP, and PAP ligands resulted in different surface basicity of modified mesoporous silica materials. The results have shown that higher basicity of the amino ligand increases the efficiency of sorbents with respect to CO₂. However, regeneration of adsorbent was faster for materials containing a ligand of lower basicity (PAP). The sorption capacities of CO₂ were 1.04 mmol/g for SBA-12/AP, 0.98 mmol/g for SBA-12/MAP, and 0.68 mmol/g for SBA-12/PAP [15].

Because CO₂ has high affinity to the amino group, grafting of ligands containing a large number of basic centers can increase the sorption capacity. Therefore, PEI was suggested as a suitable “molecular basket” for CO₂ capture. Xu et al. [7] reported that combination of MCM-41 with PEI had a synergetic effect on CO₂ adsorption. At a loading of 50 weight% of PEI the adsorption capacity was 2.55 mmol/g of adsorbent, which is higher than that of the pure PEI (2.50 mmol/g of adsorbent). When the PEI loading increased to 75 weight%, the adsorption capacity increased to 3.02 mmol/g [7].

Son et al. [16] studied different mesoporous materials (MCM-41, MCM-48, SBA-15, SBA-16, and KIT-6) impregnated by PEI. The values of adsorption capacities varied from 2.50 to 3.07 mmol/g of sorbent in the order: MCM-41 < MCM-48 < SBA-16 ≈ SBA-15 < KIT-6.

CO₂ adsorption over SBA-15 modified by PEI was studied using IR spectroscopy by Wang et al. [17]. The IR results showed that a portion of PEI was fixed on the

surface of SBA-15 through the interaction between amine groups and isolated surface silanol groups. The studies also suggested that PEI is loaded in the pores of SBA-15 in multilayers and that the sorption of CO₂ includes its sorption by PEI anchored on the surface of SBA-15 and the diffusion and sorption of CO₂ inside multilayers of PEI [17].

Separation of CO₂ from flue gas of natural-gas-fired boilers was studied by Xu et al. [18]. They investigated adsorption of CO₂ from flue gas containing CO₂, N₂, O₂, CO, H₂O, and NO_x over MCM-41 modified by PEI. The results showed that CO₂ was selectively separated from simulated flue gas. The adsorbed amount of CO₂ was around 3,000 times larger than that of NO_x.

Kumar et al. [19] studied MCM-48 membranes modified by PEI for selectivity to N₂ permeation from N₂/CO₂ mixture. The separation factor N₂/CO₂ for PEI/MCM-48 membranes increased with increasing concentration of CO₂. The highest N₂/CO₂ selectivity was observed at room temperature in the presence of ~2.6% water vapor.

It can be seen from this literature survey that several studies have been devoted to carbon dioxide sorption over PEI-modified silica [7, 16–19]. In the present work we have studied the influence of different molecular weights of PEI and the influence of different synthetic pathways (impregnation or grafting) on the properties of PEI-modified SBA-15 silica.

Results and discussion

Figure 1 shows the nitrogen adsorption/desorption isotherms of SBA-15 silica and PEI-modified materials prepared by impregnation. The isotherm of SBA-15

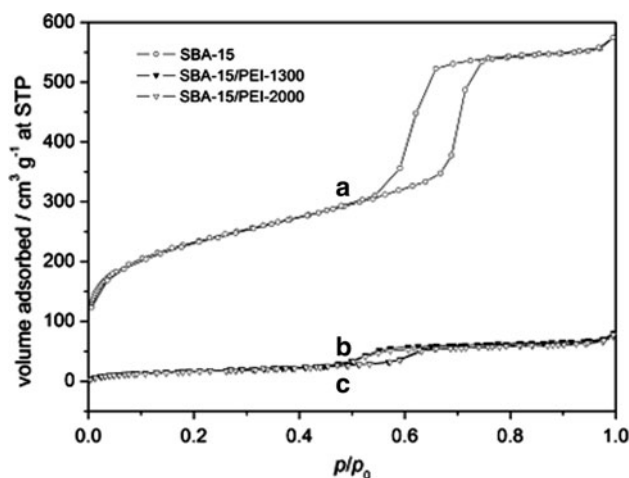


Fig. 1 Nitrogen adsorption/desorption isotherms for *a* SBA-15, *b* SBA-15/PEI-1300, and *c* SBA-15/PEI-2000 at standard temperature and pressure (STP; 273.15 K and 10⁵ Pa)

(curve a) is of type IV as classified by the International Union of Pure and Applied Chemistry (IUPAC) [20], with a hysteresis loop showing parallel adsorption/desorption branches. The initial part of the adsorption isotherm corresponds to adsorption in the micropores of SBA-15 and formation of multilayer film on the pore walls. The adsorption step in the range $p/p_0 = 0.68\text{--}0.75$ corresponds to capillary condensation. After the filling of mesopores, no additional uptake was observed at pressures $p/p_0 > 0.75$. Desorption from the SBA-15 is delayed in comparison with adsorption, and the evaporation step occurred in the range $p/p_0 = 0.66\text{--}0.58$. The hysteresis loop is relatively narrow, and adsorption/desorption branches are practically vertical, which is typical of materials possessing large, similar, and uniformly ordered two-dimensional (2D) mesopores. The Brunauer–Emmett–Teller (BET) surface area (S_{BET}) of SBA-15 sample was $799\text{ m}^2/\text{g}$; the external surface area (S_{EXT}) determined by the t -plot method was $48\text{ m}^2/\text{g}$. The average mesopore size (d) calculated by the nonlocal density functional theory (NLDFT) method was 70 \AA , and the pore volume (dV) was $0.847\text{ cm}^3/\text{g}$ (Table 1).

The mesoporosity as indicated by N_2 isotherms was further confirmed by high-resolution transmission electron microscopy (HRTEM). Figure 2 shows a view of the periodic porous structure of hexagonal symmetry typical for SBA-15. The structure consists of cylindrical channels surrounded by siliceous walls. The approximate pore size of SBA-15 as estimated from HRTEM is comparable to the values achieved from N_2 adsorption.

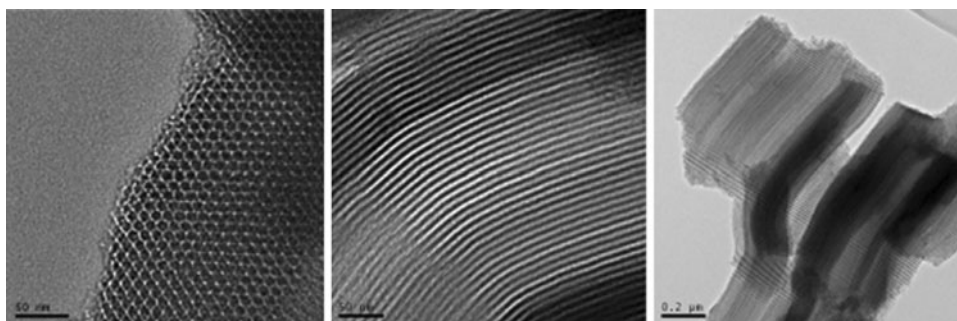
Table 1 Textural properties of unmodified and modified SBA-15

Sample	S_{BET} (m^2/g)	S_{EXT} (m^2/g)	d (\AA)	dV (cm^3/g)
SBA-15	799	48	70	0.85
SBA-15/PEI-1300	65	16	61	0.11
SBA-15/PEI-2000	63	16	61	0.10
SBA-15/Cl-PTES	508	33	66	0.59
SBA-15/Cl-PTES_PEI-1300	138	18	61	0.21
SBA-15/Cl-PTES_PEI-2000	52	13	55	0.08

The prepared and characterized SBA-15 material was used for subsequent modification by impregnation or grafting. Nitrogen adsorption/desorption isotherms of SBA-15 impregnated by PEI of different molecular weight are presented in Fig. 1 (curves b, c). The shape of the adsorption isotherms of the SBA-15/PEI-1300 and SBA-15/PEI-2000 samples is similar. The isotherms of modified samples, similarly to the isotherm of pure SBA-15, are of type IV according to the IUPAC classification. However, the capillary condensation step in modified samples is shifted to lower relative pressures, indicating lower pore size in the modified samples, due to the filling of mesopores by PEI. As can be seen in Fig. 1, curves b and c almost coincide, indicating the similar textural characteristics of the PEI-modified samples prepared by impregnation. The BET surface area of the of SBA-15/PEI-1300 and SBA-15/PEI-2000 samples was 63 and $65\text{ m}^2/\text{g}$, respectively. Values of pore volume and pore size distribution (PSD) are summarized in Table 1. By thermogravimetry analysis (TGA) it was further confirmed (see later in the text) that a similar amount of PEI-1300 and PEI-2000 was loaded into SBA-15.

The nitrogen adsorption/desorption isotherms of the samples prepared by a two-step modification procedure are presented in Fig. 3. The first step of the synthesis consisted of grafting of (3-chloropropyl)triethoxysilane (Cl-PTES) on the surface. The nitrogen adsorption/desorption isotherm of the product is shown as isotherm b in Fig. 3. A decrease of the total adsorbed volume of nitrogen was observed after grafting due to anchoring of $-\text{CH}_2-\text{CH}_2-\text{CH}_2-\text{Cl}$ chains onto the surface of SBA-15. The modification of SBA-15 by Cl-PTES leads to a decrease of surface area from the value of $799\text{ m}^2/\text{g}$ typical for SBA-15 to $508\text{ m}^2/\text{g}$ typical for SBA-15/Cl-PTES. Similarly, the pore volume decreased from the value of 0.85 to $0.59\text{ cm}^3/\text{g}$. In the second step of the modification, the PEI ligands were covalently attached on propyl chains using a procedure described elsewhere [21–23]. The reaction takes place through nucleophilic substitution of chlorine atoms by nitrogen atoms of PEI. After anchoring of PEI the total nitrogen uptake and pore size further decreased.

Fig. 2 HRTEM micrographs of SBA-15



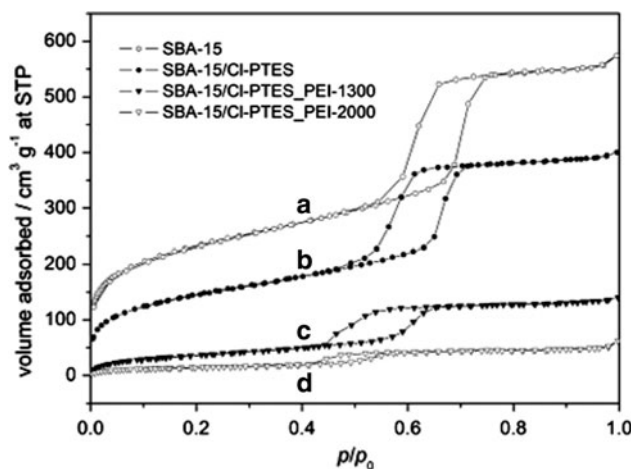


Fig. 3 Nitrogen adsorption/desorption isotherms for *a* SBA-15, *b* SBA-15/Cl-PTES, *c* SBA-15/Cl-PTES/PEI-1300, and *d* SBA-15/Cl-PTES/PEI-2000 at STP

The statistical PSD in the sample SBA-15 was centered at 70 Å. After grafting of the chloropropyl chains, the PSD of the sample decreased to 66 Å. The subsequent reaction with PEI ligands gave materials SBA-15/PEI-1300 and SBA-15/PEI-2000, with average pore size of 61 and 55 Å, respectively. The grafting of the bulkier PEI-2000 ligand onto the surface led to a greater decrease of pore size. Similarly, the surface area of SBA-15/Cl-PTES/PEI-2000 (52 m²/g) was lower compared with the surface area of SBA-15/Cl-PTES/PEI-1300 (138 m²/g). These differences probably reflect the different dimensions of PEI-1300 and PEI-2000, which result in lower pore volume and smaller pore size for SBA-15/Cl-PTES/PEI-2000.

The stability of the mesoporous SBA-15 material subjected to modification was monitored by small-angle X-ray scattering (SAXS). The SAXS pattern of SBA-15 (Fig. 4) exhibits a strong peak at $q = 0.067 \text{ \AA}^{-1}$ and weak peaks at $q = 0.116$ and 0.135 \AA^{-1} . From the SAXS patterns of PEI-modified samples it is obvious that neither impregnation nor grafting affected the porous structure of the SBA-15 matrix. The peaks in the SAXS patterns of PEI-modified samples are at similar q values to those for the parent SBA-15, confirming the similar unit cell parameter in the long-range ordering of the material (Fig. 4a, b).

The thermal stability of the prepared materials and the amount of PEI which was loaded into the porous matrix by respective procedures was measured by thermogravimetry (TG). Figure 5a shows TG/differential thermal analysis (DTA) curves of the SBA-15/PEI-1300 and SBA-15/PEI-2000 samples. In the first step of the thermal decomposition, the dehydration and thermodesorption of water from the porous structure take place, accompanied by an endothermic peak in the DTA curve with a minimum at 100 °C. The mass loss corresponding to water release was 13.76%

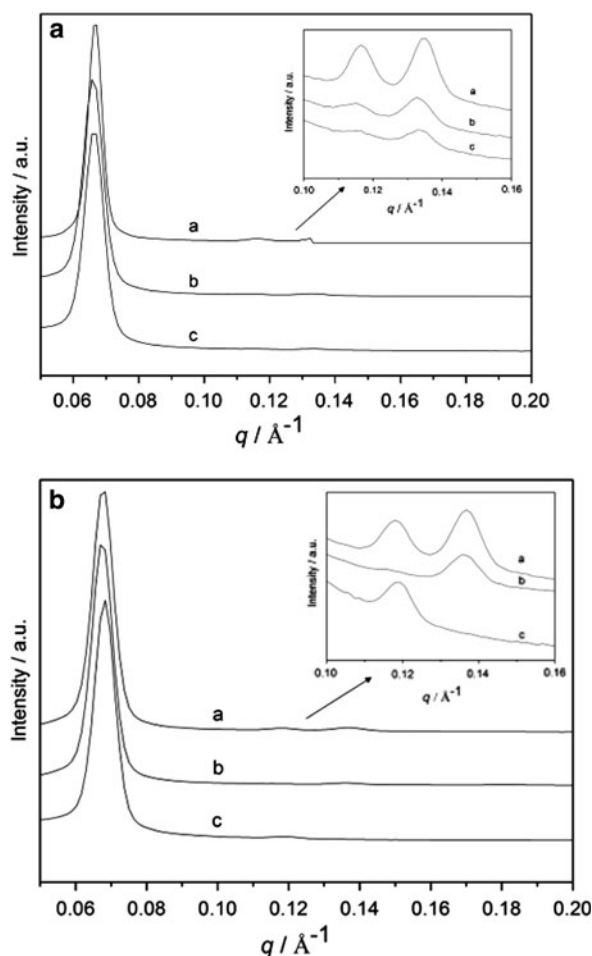


Fig. 4 SAXS patterns of the samples *a* SBA-15, *b* SBA-15/PEI-1300, and *c* SBA-15/PEI-2000. **b** *a* SBA-15/Cl, *b* SBA-15/Cl-PTES/PEI-1300, *c* SBA-15/Cl-PTES/PEI-2000

for SBA-15/PEI-1300 and 10.53% for SBA-15/PEI-2000. At higher temperatures, in the temperature range 200–800 °C, a three-step thermal decomposition of PEI takes place. This decomposition is characterized by a strong exothermic peak with maximum at 234 °C and by two weaker exothermic peaks with maxima at 351 and 640 °C for sample SBA-15/PEI-1300 and 379 and 650 °C for sample SBA-15/PEI-2000. The total mass loss due to pyrolysis of polymer chains was 33.02% for the SBA-15/PEI-1300 sample and 34.28% for the SBA-15/PEI-2000 sample. It can be seen from Fig. 5a that similar mass loss was observed for both samples, indicating that a similar amount of PEI-1300 and PEI-2000 was loaded into the pores of SBA-15 by the impregnation method. This also agrees with the similar textural characteristics (surface area, pore size, and pore volume) observed for these samples (Fig. 1; Table 1).

The thermal decomposition of the samples modified by grafting is shown in Fig. 5b. Curve *a* in Fig. 5b shows the mass change during thermal decomposition of the SBA-15/

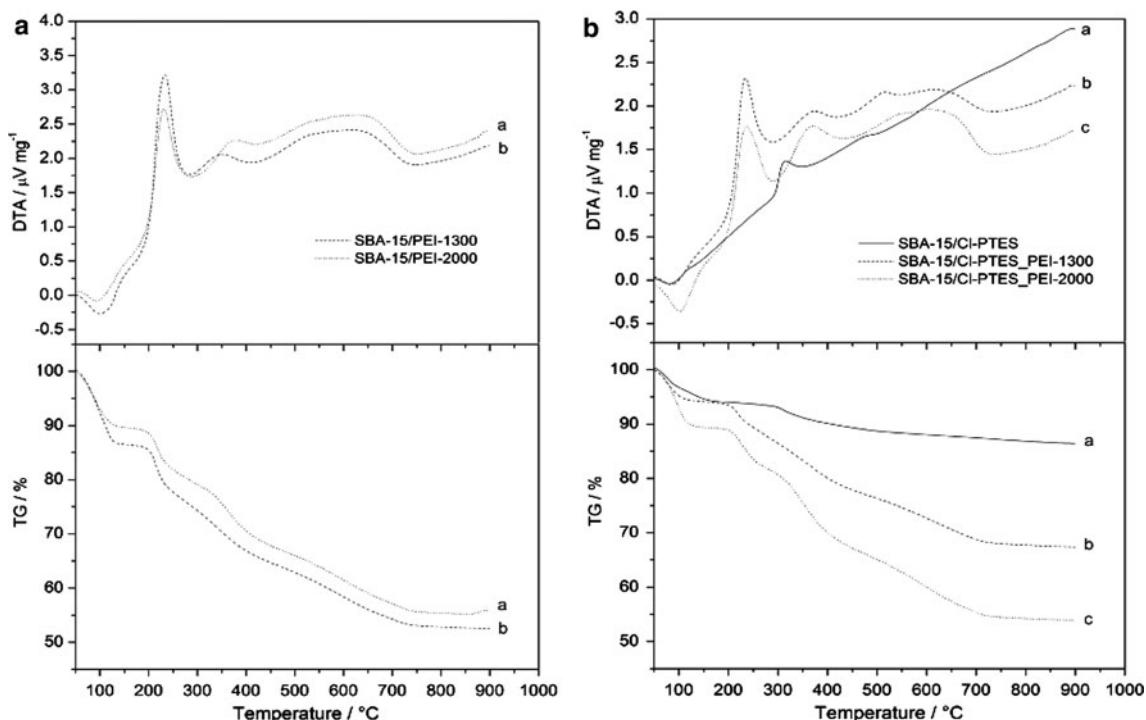


Fig. 5 TG/DTA curves of samples **a** SBA-15/PEI-1300, **b** SBA-15/PEI-2000. **b** **a** SBA-15/Cl-PTES, **b** SBA-15/Cl-PTES_PEI-1300, **c** SBA-15/Cl-PTES_PEI-2000

Cl-PTES sample. In the first step the dehydration of the sample takes place. After the dehydration, the sample is stable up to 280 °C. Above this temperature, in the range 290–500 °C, the chloropropyl chains are decomposed, accompanied by exothermic effects with maxima at 320 and 480 °C on the DTA curve. The total mass loss corresponding to the release of chloropropyl ligands is 7.58%. The thermoanalytical curves were changed after the anchoring of PEI ligands in the SBA-15/Cl-PTES_PEI-1300 and SBA-15/Cl-PTES_PEI-2000 samples (Fig. 5b, curves b, c). The decomposition of PEI-modified samples starts at lower temperature in comparison with SBA-15/Cl-PTES, due to the lower thermal stability of PEI ligands. The onset of the thermal decomposition of the SBA-15/Cl-PTES_PEI-1300 and SBA-15/Cl-PTES_PEI-2000 samples was about 240 °C. The observed mass loss corresponding to the release of the organic ligands from the SBA-15/Cl-PTES_PEI-1300 sample was 26.52%. For the SBA-15/Cl-PTES_PEI-2000 sample the corresponding value was 35.32%. The higher mass loss observed for the SBA-15/Cl-PTES_PEI-2000 sample shows the larger amount of PEI anchored on the surface of SBA-15. This is in agreement with the results of nitrogen adsorption, where lower surface area and lower pore volume were observed for the SBA-15/Cl-PTES_PEI-2000 sample. Moreover, the higher thermal stability of the samples prepared by grafting (240 °C) in

comparison with the thermal stability of the samples prepared by impregnation (200 °C) shows the successful anchoring of PEI molecules on propyl chains by the substitution reaction.

The modification of SBA-15 by PEI was also studied by Fourier-transform infrared (FTIR) spectra. The spectra of PEI-modified samples showed similar characteristics; therefore, only an illustrative example, the spectrum of the sample SBA-15/Cl-PTES_PEI-1300, is discussed in the text and displayed in Fig. 6. The peaks corresponding to stretching Si–O–Si vibrations of the silica framework were present in the IR spectra of all samples. The band of the asymmetric Si–O–Si stretch, $\nu_{as}(\text{Si–O–Si})$, was observed at about 1,080 cm^{-1} and the band of the symmetric Si–O–Si stretch, $\nu_s(\text{Si–O–Si})$, was observed at about 800 cm^{-1} . The deformation vibration $\delta(\text{Si–O–Si})$ was observed at 460 cm^{-1} . The band at 1,630 cm^{-1} corresponds with bending vibration of physisorbed water.

The modification of the silica by organic groups was reflected in the spectrum of the SBA-15/Cl-PTES sample by the presence of asymmetric and symmetric CH_2 stretches at 2,960 and 2,848 cm^{-1} . Moreover, a weak band corresponding to the $\delta(\text{CH}_2)$ vibration of $\text{Cl–CH}_2\text{–CH}_2\text{–CH}_2$ ligands was observed at 1,457 cm^{-1} . The anchoring of PEI chains on the surface of SBA-15 was reflected in the IR spectra by $\nu(\text{N–H})$ stretching at 3,058 cm^{-1} , bending

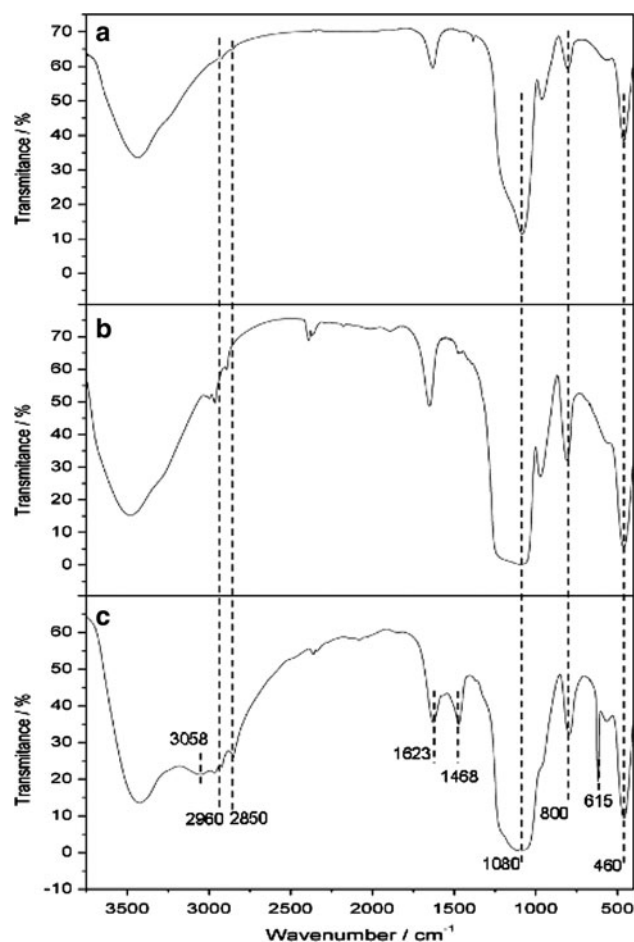


Fig. 6 FTIR spectra of the samples **a** SBA-15, **b** SBA-15/Cl-PTES, and **c** SBA-15/Cl-PTES-PEI-1300

vibration of CH_2 groups at $1,468\text{ cm}^{-1}$, and a band of $\gamma(\text{C-H})$ vibration at 615 cm^{-1} (Fig. 6c). The lower value of $\nu(\text{N-H})$ stretching vibration may indicate the presence of hydrogen bonding, or formation of ammonium carbamates and alkylammonium ions due to reaction of amine active sites of PEI with carbon dioxide from air (see Eq. 1 below) [11, 14, 17, 19, 24]. Similarly, the value of the bending vibration of physisorbed water ($1,623\text{ cm}^{-1}$) is downshifted in the spectrum of the SBA-15/Cl-PTES-PEI-1300 sample in comparison with this band in the spectrum of SBA-15 ($1,630\text{ cm}^{-1}$), probably due to hydrogen bonding between H_2O and PEI ligands.

Sorption of carbon dioxide

Carbon dioxide sorption was investigated by gravimetric method at 303 K . The results of the sorption studies are shown in Fig. 7. The flow of CO_2 over the samples led to a weight gain as reflected by the TGA curve and to the evolution of heat as reflected by an exothermic effect on the DTA curve. The observed exothermic effect is due to

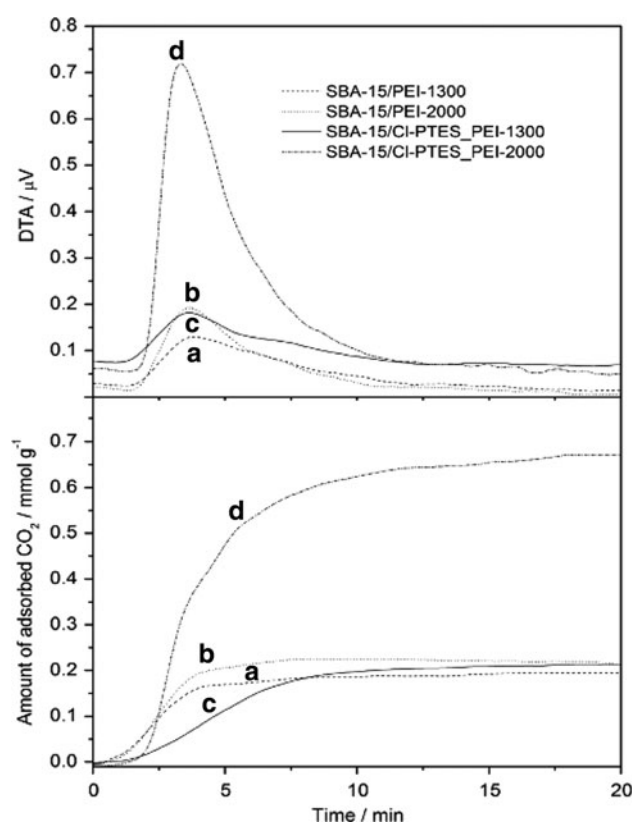
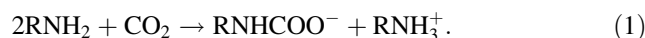


Fig. 7 Carbon dioxide sorption over the samples **a** SBA-15/PEI-1300, **b** SBA-15/PEI-2000, **c** SBA-15/Cl-PTES-PEI-1300, and **d** SBA-15/Cl-PTES-PEI-2000

interaction between carbon dioxide and amine groups of PEI, leading to the formation of carbamate (Eq. 1) [14, 19, 24].



The amount of adsorbed CO_2 was 0.19 mmol/g for SBA-15/PEI-1300, 0.22 mmol/g for SBA-15/PEI-2000, 0.21 mmol/g for SBA-15/Cl-PTES-PEI-1300, and 0.67 mmol/g for SBA-15/Cl-PTES-PEI-2000. The determined sorption capacity was lower than observed in other works for PEI-modified materials [7, 16]. The lower value may result from the method used for desorption studies, as it is well known that TGA may underestimate actual CO_2 uptake [25]. However, the low values observed for impregnated samples suggest that probably surface adsorption occurred and the active sites inside the pores are poorly accessible for carbon dioxide molecules. As was suggested [17], PEI is organized into multiple layers in the porous matrix. In the samples prepared by impregnation, the large loading of PEI into the porous matrix and the filling of the pores may hinder diffusion of CO_2 inside such layers and, consequently, the observed CO_2 uptake is mainly due to surface adsorption. When the samples were prepared by grafting, the assembly of the PEI molecules into the layers is violated, and the amine active sites may be more accessible to CO_2 . Consequently, higher uptake

was observed for grafted samples. SBA-15/Cl-PTES_PEI-2000 showed higher sorption capacity (0.67 mmol/g) than SBA-15/Cl-PTES_PEI-1300 (0.21 mmol/g), which may reflect the higher density of active centers available for sorption of carbon dioxide in SBA-15/Cl-PTES_PEI-2000 in comparison with SBA-15/Cl-PTES_PEI-1300.

Figure 8 shows three cyclic sorption measurements for the SBA-15/Cl-PTES_PEI-2000 sample. After each sorption step the sample was regenerated by heating at 70 °C for 30 min. It can be seen that carbon dioxide can be adsorbed over the sample repeatedly without loss of sorption capacity and that the sorbent can be easily regenerated under mild conditions. From the studies of carbon dioxide adsorption on amine-modified silica materials it is known that the heat of adsorption of carbon dioxide is about 70 kJ/mol [26, 27]. Therefore the interaction between carbon dioxide and amine is stronger than physisorption and leads to the formation of carbamates. However, the energy of such interaction is lower than the energy of covalent bonds, which can explain the easy regeneration and reversibility of the reaction.

Conclusions

Mesoporous silica SBA-15 was modified by PEI by two methods (impregnation and grafting) and tested as a sorbent for carbon dioxide. Characterization of the prepared samples by nitrogen adsorption/desorption, thermal analysis, SAXS, and infrared spectroscopy confirmed successful modification of the SBA-15 silica by PEI ligands without loss of periodicity of the SBA-15 matrix. The study of carbon dioxide adsorption over the prepared samples showed that higher sorption capacity was observed for samples prepared by grafting. The largest adsorbed amount

(0.67 mmol/g) was observed for SBA-15/Cl-PTES_PEI-2000. It was suggested that, in samples prepared by impregnation, PEI may be organized into multiple layers, which may hinder diffusion of CO₂ to amine active sites. Moreover, it was shown that the prepared materials can be regenerated under mild conditions by heating to 343 K.

Experimental

All chemicals were purchased from Sigma–Aldrich and used without further purification. Toluene was dried over molecular sieves before synthesis. Tetraethoxysilane (TEOS) was used as silica source and Pluronic P123 [(EO)₂₀(PO)₇₀(EO)₂₀; EO = –CH₂CH₂O–, PO = –CH₂(CH₃)CHO–] as a structure directing agent. PEI of different molecular weights (1,300 and 2,000 g mol^{–1}) was used for impregnation, and (3-chloropropyl)triethoxysilane was used for grafting of the silica.

Preparation of SBA-15 mesoporous silica

Mesoporous silica SBA-15 was synthesized by a conventional procedure using nonionic surfactant Pluronic P123. Pluronic P123 (8.0 g) was dissolved in 60 g distilled water and 240 g 2 M HCl solution with stirring at 35 °C, and 17 g of TEOS was then added. The resulting mixture was stirred at 35 °C for 20 h and then aged at 80 °C for 24 h. The solid product was recovered by filtration and dried at room temperature. The organic template was removed by calcination in air at 500 °C for 7 h.

Preparation of imine-modified SBA-15

The surface modification of mesoporous silica SBA-15 by PEI was carried out by two methods. The first method consisted of impregnation of SBA-15 with PEI [7]. PEI (3 cm³) was dissolved in 16 g methanol under stirring for about 15 min. Then, 0.7 g SBA-15, which was dehydrated at 150 °C for 1 h, was added. The resultant solution was continuously stirred for 1 h. The final solid materials were recovered by filtration and dried at laboratory temperature. The second procedure was a two-step modification including grafting of SBA-15 by Cl-PTES, followed by substitution of chlorine atoms by PEI ligands. At the beginning of grafting SBA-15 by PEI, SBA-15 was dehydrated at 150 °C for 1 h to remove adsorbed moisture. Then 4.35 g SBA-15 was dispersed in 200 cm³ dried toluene, and 13 cm³ Cl-PTES was added to the suspension, which was further kept under reflux for 24 h. The solid product was recovered by filtration, washed out with toluene, and dried at laboratory temperature. Then, 500 mg SBA-15/Cl-PTES was dispersed in 50 cm³ ethanol, and

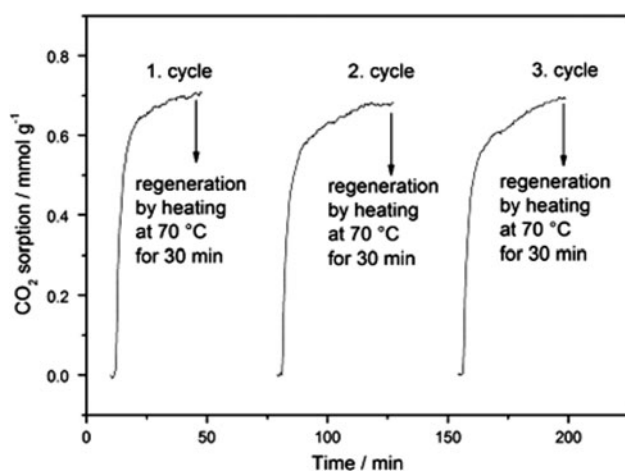


Fig. 8 Adsorption cycles of carbon dioxide studied by TG at 303 K on the SBA-15/Cl-PTES_PEI-2000 sample

2 cm³ PEI (PEI-1300 or PEI-2000) was added to the suspension. The suspension was refluxed for 24 h. The final solid product was recovered by filtration, washed out with ethanol, and dried at room temperature.

Characterization of prepared sorbents

Nitrogen adsorption/desorption experiments were performed at 77 K by using a Quantachrome Nova 1200 instrument. Prior to adsorption, samples were degassed at 110 °C for 24 h. Textural characteristics and PSD of all samples were determined by adsorption/desorption of nitrogen. The specific surface areas of the samples were calculated by Brunauer–Emmett–Teller equations in a pressure range (0.05–0.30), and PSD of the samples was calculated by the NLDFT method. Long-range ordering was reflected by small-angle X-ray scattering (SAXS) experiments which were measured at the B1/Jusifa Hasylab beamline (DESY Hamburg) with beam energy of 12 keV ($\lambda = 1.03 \text{ \AA}$). HRTEM micrographs were taken using a JEOL JEM 3010 microscope. Infrared spectra were recorded using an Avatar FTIR spectrometer. Thermal stability was evaluated using a STA Netzsch 409PC apparatus under dynamic conditions with heating rate of 9 °C/min in air. Sorption of CO₂ was determined by using a thermogravimetric balance Netzsch 409PC at 303 K. Prior to the sorption studies, the samples were heated at 343 K for 30 min.

Acknowledgments This work was supported in part by the European Community STREP project “DeSANNS” (no. FP6-SES6-020133), the Slovak Research and Development Agency under contract RPEU-0027-06 (OrNaMat), the VEGA project (no. 1/0119/08) of the Ministry of Education of the Slovak Republic, and grant VVGS PF 14/2009/CH. The ERDF EU (Operational Program “Research and Development” financed through European Regional Development Fund) grant, under contract ITMS 26220120019 (Centre of Excellence of Advanced Materials with Nano, and Submicron, Structure) is also gratefully acknowledged. The authors thank Dr. U. Vainio (DESY/Hasylab, Hamburg, Germany) for assistance at the B1 beamline and Dr. N. Murafa (IIC AS CR, Rez, Czech Republic) for TEM measurements.

References

1. Cantarel A, Bloor JMG, Jean-François S (2009) IOP Conf Ser Earth Environ Sci 6:242044

2. Cox PM, Betts RA, Jones CD, Spall SA, Totterdell IJ (2000) Nature 408:184
3. Cramer W, Bondeau A, Woodward FI, Prentice IC, Betts RA, Brovkin V, Cox PM, Fisher V, Foley JA, Friend AD, Kucharik C, Lomas MR, Ramankutty N, Sitch S, Smith B, White A, Young-Molling C (2001) Glob Chang Biol 7:357
4. Matthews HD, Gillett NP, Stott PA, Zickfeld K (2009) Nature 459:829
5. Ledley TS, Sundquist ET, Schwartz SE (1999) Eos Trans AGU 80:453
6. Xu X, Song Ch, Miller BG, Scaroni AW (2005) Ind Eng Chem Res 44:8133
7. Xu X, Song C, Andréßen J, Miller BG, Scaroni AW (2003) Microporous Mesoporous Mater 62:29
8. Wong S, Bioletti R (2002) Carbon dioxide separation technologies, carbon & energy management alberta research council. Edmonton, Alberta
9. Veaweb A, Tontiwachwuthikul P, Chakma A (1999) Ind Eng Chem Res 38:3917
10. Chakma A (1997) Energy Conversat Manage 38:S51
11. Leal O, Bolivar C, Ovalles C, Garcia JJ, Espidel Y (1995) Inorg Chim Acta 240:183
12. Huang HY, Yang RT, Chinn D, Munson CL (2003) Ind Eng Chem Res 42:2427
13. Hiyoshi N, Yogo K, Yashima T (2004) Stud Surf Sci Catal 154:2995
14. Kim S, Ida J, Gulians VV, Lin JYS (2005) J Phys Chem B 109:6287
15. Zeleňák V, Halamová D, Gaberová L, Bloch E, Llewellyn P (2008) Microporous Mesoporous Mater 116:358
16. Son W, Choi J, Ahn W (2008) Microporous Mesoporous Mater 113:31
17. Wang X, Schwartz V, Clark JC, Ma X, Overbury SH, Xu X, Song C (2009) J Phys Chem C 113:7260
18. Xu X, Song C, Miler BG, Scaroni AW (2005) Fuel Process Tech 86:1457
19. Kumar P, Kim S, Ida J, Gulians VV (2008) Ind Eng Chem Res 47:201
20. Sing KSW, Everett DH, Haul RAW, Moscou L, Pierotti RA, Rouquérol J, Siemieniowska T (1985) Pure Appl Chem 57:603
21. Yoshitake H, Koiso E, Horie H, Yoshimura H (2005) Microporous Mesoporous Mater 85:183
22. Gao B, An F, Liu K (2006) Appl Surf Sci 253:1946
23. Xu Q, Dong W, Li H, Li L, Feng S, Xu R (2003) Solid State Sci 5:777
24. Zheng F, Tran DN, Busche BJ, Fryxell GE, Addleman RS, Zemanian TS, Aardahl CL (2005) Ind Eng Chem Res 44:3099
25. Serna-Guerrero R, Dana E, Sayari A (2008) Ind Eng Chem Res 47:9406
26. Knöfel C, Descarpentries J, Benzaouia A, Zeleňák V, Mornet S, Llewellyn PL, Hornebecq V (2007) Microporous Mesoporous Mater 99:77
27. Khatri RA, Chuang SSC, Soong A, McMahan G (2005) Ind Eng Chem Res 44:3702